Computational Characterization of Substrate Binding and Catalysis in *S*-Adenosylhomocysteine Hydrolase†

Yongbo Hu,*,‡ Xiaoda Yang,‡,§ Daniel H. Yin,‡,|| Janaki Mahadevan,⊥ Krzysztof Kuczera,⊥ Richard L. Schowen,‡,⊥ and Ronald T. Borchardt‡

Departments of Pharmaceutical Chemistry, Chemistry, and Molecular Biosciences, The University of Kansas, Lawrence, Kansas 66045-2106

Received August 15, 2001

ABSTRACT: *S*-Adenosylhomocysteine (AdoHcy) hydrolase catalyzes the reversible hydrolysis of AdoHcy to adenosine (Ado) and homocysteine (Hcy), playing an essential role in modulating the cellular Hcy levels and regulating activities of a host of methyltransferases in eukaryotic cells. This enzyme exists in an open conformation (active site unoccupied) and a closed conformation (active site occupied with substrate or inhibitor) [Turner, M. A., Yang, X., Yin, D., Kuczera, K., Borchardt, R. T., and Howell, P. L. (2000) *Cell Biochem. Biophys. 33*, 101−125]. To investigate the binding of natural substrates during catalysis, the computational docking program AutoDock (with confirming calculations using CHARMM) was used to predict the binding modes of various substrates or inhibitors with the closed and open forms of AdoHcy hydrolase. The results have revealed that the interaction between a substrate and the open form of the enzyme is nonspecific, whereas the binding of the substrate in the closed form is highly specific with the adenine moiety of a substrate as the main recognition factor. Residues Thr57, Glu59, Glu156, Gln181, Lys186, Asp190, Met351, and His35 are involved in substrate binding, which is consistent with the crystal structure. His55 in the docked model appears to participate in the elimination of water from Ado through the interaction with the 5′-OH group of Ado. In the same reaction, Asp131 removes a proton from the 4′ position of the substrate after the oxidation−reduction reaction in the enzyme. To identify the residues that bind the Hcy moiety, AdoHcy was docked to the closed form of AdoHcy hydrolase. The Hcy tail is predicted to interact with His55, Cys79, Asn80, Asp131, Asp134, and Leu344 in a strained conformation, which may lower the reaction barrier and enhance the catalysis rate.

S-Adenosylhomocysteine (AdoHcy)[1] is a product inhibitor of enzymes that catalyze transfer of the methyl group from *S*-adenosylmethionine (AdoMet) to a variety of recipient molecules (*1*). In eukaryotic cells, the only known pathway for the catabolism of AdoHcy is reversible hydrolysis to adenosine (Ado) and homocysteine (Hcy) catalyzed by AdoHcy hydrolase (EC 3.3.1.1). The enzyme contains a tightly bound NAD^+/NADH cofactor which undergoes redox cycling during the catalytic reaction (Figure 1). Inhibitors of AdoHcy hydrolase have been shown to produce antiviral and antiparasitic effects because of the key role of the enzyme in the regulation of all AdoMet-dependent transmethylation reactions (*2*−*5*). In humans, elevated plasma levels of Hcy, the hydrolysis product of AdoHcy, have been implicated as a risk factor for cardiovascular disease (*6*). Therefore, AdoHcy hydrolase is of great interest as a target for the design of potential antiviral and antiparasitic agents as well as therapeutic inhibitors that may adjust the plasma Hcy levels.

Understanding the structure and catalytic mechanism of AdoHcy hydrolase is of utmost fundamental importance and is crucial for the rational design of specific structure-based and mechanism-based inhibitors. The elucidation of two crystal structures of AdoHcy hydrolase isoforms from human and rat, the sequences of which are 97% identical, has provided important details regarding the catalytic mechanism (*7*, *8*). As shown in Figure 1, the rat enzyme was crystallized in the substrate-free NAD^+ form. The human enzyme was treated with 2′,3′-dihydroxycyclopent-4′-enyladenine (DHCeA), which was bound and oxidized, arresting the enzyme in the NADH state.

Both enzymes have a homotetrameric structure with each monomer consisting of two large domains and a small C-terminal domain. The two large domains contain the binding site for the substrate and for the cofactor. The two domains are linked by a hinge. Comparison of the two crystal structures indicates large differences in the enzyme conformation (Figure 2). The substrate-free, NAD^+ form exists in

† This work was supported by National Institutes of Health Grant GM29332. Y.H. is a postdoctoral fellow of the Arthritis Foundation, and D.H.Y. is a postdoctoral fellow of the American Heart Association.

* To whom correspondence should be addressed. Phone: (785) 864-4825. Fax: (785) 864-5736. E-mail: ybhu@ku.edu.

‡ Department of Pharmaceutical Chemistry.

§ Current address: Department of Chemical Biology, School of Pharmaceutical Sciences, Peking University Health Science Center, Beijing 100083, China.

|| Current address: Department of Vaccine Pharmaceutical Research, Merck Research Laboratories, West Point, PA 19486.

⊥ Departments of Chemistry and Molecular Biosciences.

[1] Abbreviations: Ade, adenine; Ado, adenosine; AdoHcy, *S*-adenosylhomocysteine; AdoMet, *S*-adenosylmethionine; DHCe, 2′,3′-dihydroxycyclopentene; DHCeA, 2′,3′-dihydroxycyclopent-4′-enyladenine; Hcy, homocysteine; Ad, adenyl; PDB, Protein Data Bank, Research Collaboratory for Structural Bioinformatics.

10.1021/bi015690d CCC: $20.00
Published on Web 11/21/2001

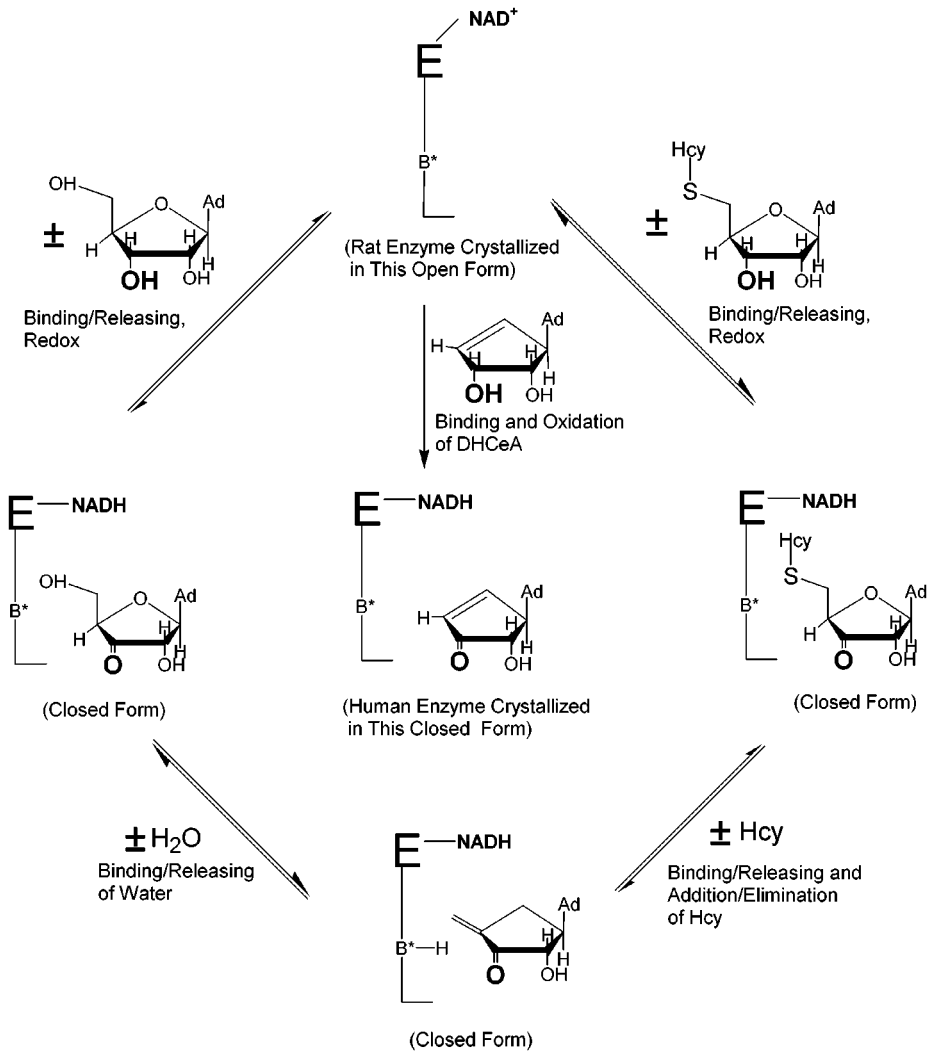

FIGURE 1: Scheme showing the catalytic cycle of AdoHcy hydrolase and forms in which enzymes were crystallized. B* stands for the base that removes the 4′ proton of the substrate during the reaction.

an "open" structure in which the two large domains are separated by a cleft. The inhibitor-bound, NADH form exists in a "closed" structure in which the two large domains have come together with the oxidized inhibitor deeply engulfed at their interface, with a "tunnel" connecting the bound inhibitor and the outside solvent. These two structures show that a large domain movement can occur with the enzyme. The speed of the domain movement in the solution has been determined by fluorescence anisotropy measurements (*9*). The fluorescence study has also shown that the binding of substrates stabilizes the enzyme in the closed conformation.

The two structures leave some important questions unanswered. Because the active site is empty in the structure of the open form of the enzyme, the nature of substrate binding in this form is unknown. For the closed structure, because DHCeA lacks the Hcy moiety, the structure does not specify the binding site for the Hcy part of the substrate. Also, the presence of the cyclopentene ring of the inhibitor in place of the ribose of Ado or AdoHcy at the catalytic site prevented an unambiguous identification of the residues involved in catalysis, because the different partial charge and ring puckering might result in a different binding conformation. For instance, the base that accepts and donates a proton at C4′ of the substrate during the redox cycle has not been identified (Figure 1).

To answer such questions, we docked various substrates and inhibitors to the open and closed forms of AdoHcy hydrolase, making use of two widely used computer simulation software packages, AutoDock and CHARMM (*10*, *11*). AutoDock employs a Monte Carlo simulated annealing technique for configurational exploration with a rapid energy evaluation using grid-based molecular affinity potentials. It has been proven to be a powerful approach for prediction of the interaction of ligands with macromolecular targets and has led to considerable success, particularly in the field of computer-aided drug design (*12*−*14*). The CHARMM molecular modeling package (*11*, *15*, *16*) was used as a supplemental approach for exploring the docking of small ligands to AdoHcy hydrolase to test the AutoDock findings. Unlike AutoDock, which allows only selected torsional rotations for the ligands, the CHARMM simulations permit ligands to freely undergo internal deformations such as bond stretching, angle bending, and dihedral distortions.

EXPERIMENTAL PROCEDURES

Software. Docking calculations were performed with the AutoDock program (version 2.4) and the CHARMM molecular modeling package (*10*, *11*, *15*, *16*). The Insight II package (BIOSYM/Molecular Simulations, San Diego, CA) was used for model building and energy minimization of

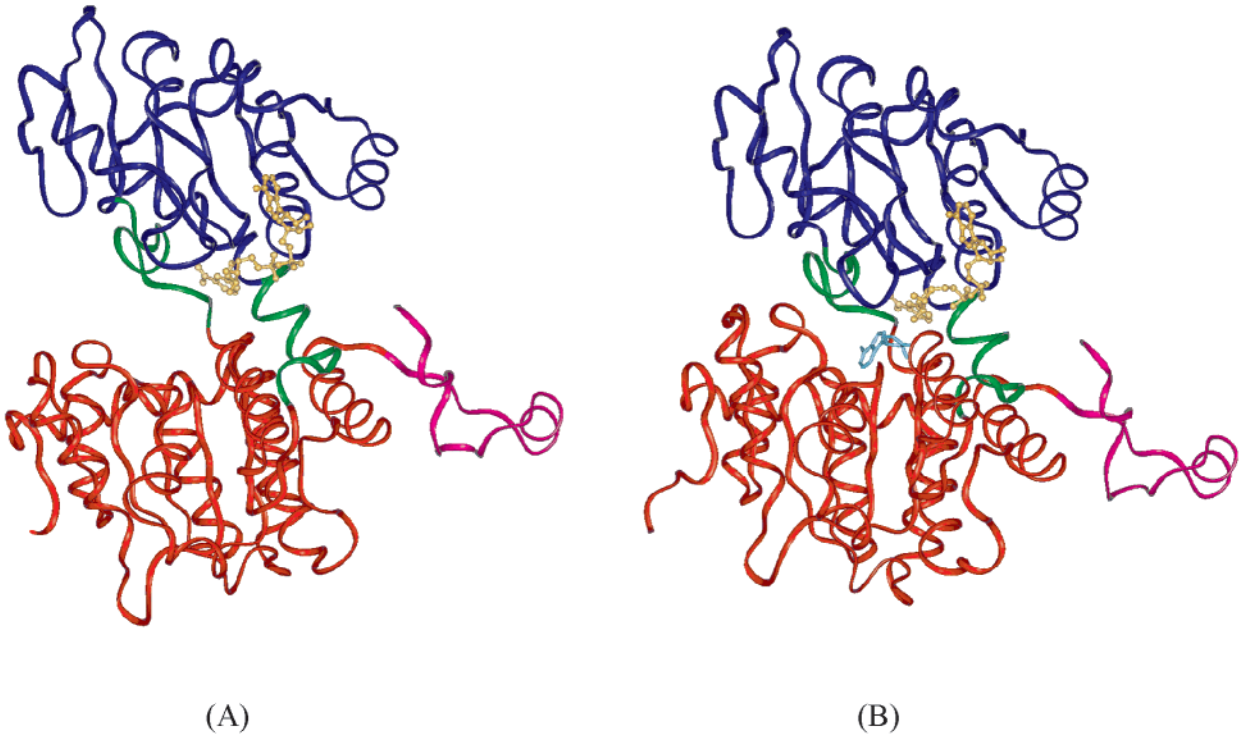

FIGURE 2: Domain structures of AdoHcy hydrolase as seen in the open (A) and closed (B) forms of the enzyme. The two large domains contain the binding site for the substrate (bottom, red domain; the inhibitor is shown in cyan) and for the cofactor (top, blue domain; the cofactor is shown in gold). The two domains are linked by a hinge (green). The smaller C-terminal domain (magenta) extends into the neighboring monomeric subunit and forms part of the cofactor (gold) binding site. The C-terminal domain of the second subunit likewise extends into the subunit that is shown and forms part of the cofactor binding site. In the closed form of the enzyme, the two large domains have moved through an angle of 17° to bring their surface structures into contact and the cofactor and substrate into proximity. A tunnel connecting the active site to the external solution allows exit and entrance of Hcy and perhaps water.

initial ligand structures. Insight II was also used to generate missing hydrogen atoms and assign partial charges for protein targets used in AutoDock runs. Properties of hydrogen bonds between ligands and the protein were calculated using Insight II and CHARMM. Mutations of amino acids involved in substrate binding in AdoHcy hydrolase were carried out using the program package Insight II. The superimposition of the catalytic domains in the open and closed forms of AdoHcy hydrolase was performed using the QUANTA program package (BIOSYM/Molecular Simulations). Structural figures were generated with MolScript and Raster3D (*17*−*19*).

Protein Coordinates. Structures of Protein Data Bank (PDB) entries 1A7A (*7*) and 1B3R (*8*) were used for the docking simulations of AdoHcy hydrolase in the closed and open forms, respectively. The 1A7A structure contains two crystallographically independent subunits of human placental AdoHcy hydrolase, with each subunit complexed with a NADH and an inhibitor 3′-keto-DHCeA completely buried in the protein interior. To generate a docking target with a substrate accessible binding cavity, the NAD^+ binding domain (residues 194−342) and the small C-terminal domain (residues 405−432), which are not directly involved in the binding of the inhibitor 3′-keto-DHCeA, were removed. Only the catalytic domain and the hinge part (residues 2−193 and 343−404, respectively, red and green regions in Figure 2) of a single subunit of the enzyme were therefore used as the target. A water molecule is also located in the active site of this structure, appearing to bridge the interaction between C4′ of 3′-keto-DHCeA and the basic sites of the side chains of His55 and Asp131. However, no such water molecule was observed in the recently determined crystal structure of human AdoHcy hydrolase complexed with neplanocin A, where the space occupied by the water in the 1A7A structure is occupied by the 5′-hydroxyl group of neplanocin A (unpublished data, communication from P. Lynne Howell, Hospital for Sick Children, Toronto, ON). Thus, the water molecule was included in the docking target only for the docking simulations of 3′-keto-DHCeA and 3′-keto-DHCe, but not for the simulations of the binding of Ado and AdoHcy, which possess 5′-hydroxyl groups.

In the 1B3R structure, four crystallographically independent subunits of rat liver AdoHcy hydrolase are represented, each with an NAD^+ cofactor and no substrate. Because of the open conformation, which allowed free access to the active site by the substrates, an entire subunit of the rat enzyme in the open form was used for the docking. For easier comparison, residue numbers for the human enzyme are used for both enzymes throughout this paper.

Ligand Coordinates. For AutoDock runs, the starting geometry of the 3′-keto-DHCeA was taken from PDB entry 1A7A. Other ligands were overlaid on the 3′-keto-DHCeA to allow similar starting coordinates to be used. Prior to docking runs, all ligand structures were placed arbitrarily ∼30 Å from the surface of the AdoHcy hydrolase. For CHARMM energy minimizations, the starting coordinates of the ligands were taken from the corresponding best docked structures of the AutoDock calculations.

Partial Charges. For AutoDock, the partial charges for the target and ligands were assigned with Insight II using the CVFF force field. The partial charges for the atoms of the ligands were modified so that the partial charges of the nonpolar hydrogen atoms were merged to the atoms to which

the hydrogen atom is bonded. For CHARMM simulations, the partial charges of proteins and ligands were assigned using standard CHARMM protein and/or peptide and nucleic acid parameters (*12*, *14*). For AdoHcy, a CHARMM topology file was constructed by combining methionine and adenosine models. In analogy to the CHARMM methionine model, the charge on the sulfur atom was taken to be −0.09, while the methylene groups to which it is bound were assigned charges of +0.09 on the hydrogens, −0.14 on Cγ of the Hcy tail, and −0.13 on C5′ of the ribose.

Simulation of Substrate Binding Using AutoDock. Affinity grid fields were generated first, using the auxiliary program AutoGrid. The position of Cγ of Asp131, which is spatially at the center of the active site of the crystal structure, was chosen as the center of the grids. The dimensions of the grid were 37.5 Å × 37.5 Å × 37.5 Å with grid points separated by 0.375 Å. All rotatable dihedrals in the ligands were assigned with the auxiliary program AutoTors and were allowed to rotate freely. The ligands were then docked by Monte Carlo simulated annealing. The parameters for the simulated annealing configurational search were identical for all docking jobs. Each simulated annealing run lasted 110 cycles with a starting temperature of 616 K in the first cycle and a temperature reduction factor of 0.95 per cycle. The maximum number of accepted or rejected steps per cycle was 30 000. The maximum translation step was kept constant at 0.2 Å for every cycle, but the maximum quaternion rotation step and dihedral rotation step had a reduction factor of 0.99 per cycle starting from a maximum rotation of 5.0° in the first cycle. For the search to be extensive, the program uses a multiple starting approach in combination with a time-dependent random number generator. The maximum allowed number of runs was set as 128.

After docking had been carried out, the 128 solutions that were produced were clustered in groups using a rms (root-mean-square) deviation tolerance of 0.5 Å. The clusters were also ranked according to the energies of their representative solutions, which are the lowest-energy solutions within each cluster. The solution ranked lowest in energy and the solutions with energy close to this one (≤5 kcal/mol) were considered as possible binding models.

Modeling of Substrate Binding Using CHARMM. A simplified simulated annealing protocol was used, involving the generation of a 1 ns molecular dynamics trajectory of the ligand in the field of the fixed protein at 1000 K. The 1000 structures, saved from the trajectory every 1 ps, served as starting points for energy minimization. The protein part of the system remained fixed at the experimental geometry, unless specifically noted. Harmonic constraints of the form $V_c = {}^1/_2 f(X - X_0)^2$ were applied to a part of the ligand structure to restrict the range of explored conformational space to the vicinity of the starting structure. The constrained coordinates were either atomic positions or the center of mass of a molecular fragment (e.g., the adenine ring). The force constants were in the range of 0.01−0.50 kcal mol^{-1} Å^{-2}. The set of low-energy optimized structures was then analyzed. For the 3′-keto-DHCeA inhibitor, the parameters for the adenine moiety were taken from the CHARMM version 22 nucleic acid force field (*15*). Parameters for the cyclopentene fragment were determined from ab initio calculations at the HF/6-31G* level using the program Gaussian92 (*23*). The equilibrium bond lengths and angles were taken from the HF/6-31G*-optimized geometry. Force constants for bond stretching, angle bending, and dihedral deformation were transferred from analogous coordinates in the CHARMM nucleic acid and protein force fields (*16*, *23*). Atomic charges were assigned on the basis of the Mulliken populations. Using an atom naming convention analogous to that of ribose, the atomic charges were 0.00 on C1′, 0.09 on H1′, 0.11 on C2′, 0.09 on H2″, −0.60 on O2′, 0.40 on H2′ (attached to O2′), 0.39 on C3′, −0.48 on O3′, −0.10 on C4′, 0.10 on H4′, −0.10 on C5′, and 0.10 on H5′.

Superimposition of the Catalytic Domains in the Open and Closed Forms of AdoHcy Hydrolase. The protein segments from position 2 through 193 and 343 through 404 in the open and closed Forms of AdoHcy hydrolase, which contain all of the interacting residues in the substrate binding site of the closed form, were selected and subjected to a least-squares superimposition using QUANTA.

RESULTS

The energetic and structural results of AutoDock and CHARMM computational experiments yield information about preferred binding modes and the specificity of binding (strength of preference for a particular mode) in the following way.

In our AutoDock protocol, each experiment consisted of 128 annealing simulations, with each simulation producing a single final structure or *solution*. The 128 solutions were first sorted in terms of the similarity of the structures; the set of solutions having a rms deviation in atomic positions of less than 0.5 Å was designated a *cluster*. If the total number of clusters generated is small, the experiment indicates strong or large *specificity of binding*, with all of the solutions resembling one of only a small number of different binding conformations and orientations. On the other hand, if the total number of clusters is large, the experiment indicates a weak or low specificity of binding, since the solutions tend to sort into many different binding conformations or orientations.

To obtain information about the nature of the preferred structures, the solutions within each cluster were ranked energetically, and the clusters were ranked by the lowest energy of the solution within them. The lowest-energy solution of the lowest-energy cluster, and all solutions with energies higher by <5.0 kcal/mol, were accepted as possible structures of the enzyme−ligand complex.

Our use of the CHARMM approach consisted of collecting a structure every picosecond from a 1 ns molecular dynamics simulation, having the lowest-energy AutoDock structure as the starting point. Thus, 1000 structures were generated. Each of these structures was then energy-minimized to obtain an optimized structure. The lowest-energy structures from the set of 1000 were then compared to the structures obtained in the AutoDock procedure. The actual numerical energies used in the ranking procedure differ between AutoDock and CHARMM and should be regarded merely as scoring systems, rather than realistic estimates of interaction energies. In the considerations below, qualitative and semiquantitative energetic comparisons within the AutoDock formalism or the CHARMM formalism are utilized, but cross comparisons are not made.

Tests of the Methods. As a preliminary test of the methods, the inhibitor 3′-keto-DHCeA was docked into the closed form

Table 1: AutoDock Docking Results for 3′-Keto-DHCeA with Mutants of AdoHcy Hydrolase as the Targets

protein[a]	no. of clusters[b]	no. of members in the lowest-energy cluster
wild type	16	50
T57A	**45**	**30**
E59A	**51**	**38**
E156A	20	44
N181A	22	40
K186A	24	45
D190A	18	46

[a] T57 and E59 interact with adenine ring in the 1A7A crystal structure; the rest interact with the 3′-keto-DHCe moiety. [b] Clustering of a total of 128 runs.

of human AdoHcy hydrolase with two different programs, AutoDock and CHARMM. With AutoDock, 128 Monte Carlo runs produced 16 clusters; the lowest-energy cluster contained 36 solutions (Table 1). The rms deviation between the lowest-energy solution ($E = -49.82$ kcal/mol) and the crystal structure was 0.82 Å. CHARMM simulations were performed with a weak constraint on the adenine center of mass ($f = 0.01$ kcal mol^{-1} Å^{-2}) as described in Experimental Procedures. The two most stable complexes had energies of −60.72 and −60.67 kcal/mol, respectively. These structures were found 299 and 266 times, respectively, among the 1000 minima generated by the simulated annealing procedure. In both cases, the rms deviation of the adenine fragment from the position in the 1A7A crystal structure was less than 1.6 Å. The contacts of the adenine moiety of 3′-keto-DHCeA in the AutoDock and CHARMM models were identical to those in the crystal structure, involving residues Thr57, Glu59, Met351, and His353 (*7*). The residues interacting with the 3′-C═O and 2′-OH groups of the inhibitor were also the same as in the crystal structure: Glu156, Gln181, Lys186, and Asp190.

Since Thr57, Glu59, Glu156, Gln181, Lys186, and Asp190 of AdoHcy hydrolase are the key residues involved in 3′-keto-DHCeA binding, mutations of these residues should affect the binding specificity of the inhibitor. To validate the docking methods as measures of binding specificity, 3′-keto-DHCeA was docked into mutant proteins T57A, E59A, E156A, N181A, K186A, and D190A, which were computationally generated with the methods described above. The simulations of docking of 3′-keto-DHCeA into the mutants T57A and E59A produced 45 and 51 clusters, respectively, indicating a strong reduction in specificity. Simulations using E156A, N181A, and K186A as the targets produced a modest loss of specificity (20, 22, and 24 clusters, respectively, instead of 16). The D190A mutation generated only a small loss of specificity (18 vs 16 clusters).

Docking of Ado and AdoHcy to the Open Form of AdoHcy Hydrolase. The substrates Ado and AdoHcy were docked into the open form of AdoHcy hydrolase using the complete subunit A of the rat protein crystal structure (PDB entry 1B3R) as the target. For both substrates, a large number of clusters were produced (Table 2). One hundred twenty-eight runs yielded 106 clusters for Ado and 120 for AdoHcy, with docked ligands exhibiting a wide range of rms deviations (5−33 Å). The minimum energy structures for Ado and AdoHcy had total interaction energies of −42.9 and −67.8 kcal/mol, respectively, which are significantly higher than the energies calculated for the docking of these two substrates

Table 2: AutoDock Docking Results for Various Ligands with the Open and Closed Forms of AdoHcy Hydrolase as the Targets

	open form		closed form	
	no. of clusters[a]	lowest energy[b] (kcal/mol)	no. of clusters[a]	lowest energy[b] (kcal/mol)
Ado	106	−42.9	22	−62.0
AdoHcy	120	−67.8	26	−93.2
adenine			10	−37.1
3′-keto-DHCe			33	−26.8

[a] Clustering of a total of 128 runs. [b] Scoring function energy of the lowest-energy solution of the lowest-energy cluster.

in the closed structure (−62.0 kcal/mol for Ado and −93.2 kcal/mol for AdoHcy, as the result presented below). These results suggest that the substrates bind to the open form of the enzyme nonspecifically and weakly.

CHARMM docking simulations of Ado and AdoHcy to the open form were also performed, with fully flexible ligands and a partially flexible target (side chains allowed to reorient). After the protein hydrogen atoms had been built in, a 1 ns trajectory of the fully flexible zwitterionic AdoHcy ligand moving in the field of the rigid enzyme was generated at 3000 K. The centers of mass of the adenine moieties of Ado and AdoHcy were constrained by a harmonic force constant f of 0.5 kcal mol^{-1} Å^{-2} so that they remained close to a reference point located as follows. The substrate-binding domain of the closed form of the enzyme (PDB entry 1A7A), including the structure of 3′-keto-DHCeA, was overlaid on the corresponding domain of the open form of the enzyme (PDB entry 1A7A). The center of mass of 3′-keto-DHCeA then defined the reference point.

In all CHARMM simulations, a wide range of possible docked structures was found in the general area of the active site. This is in agreement with the AutoDock results and indicates a low specificity for substrate binding in the open form. The minimum energy structure for Ado as a ligand was obtained with protein side chains relaxed. Several of the contacts found in the crystal structure of the inhibitor 3′-keto-DHCeA bound to the closed form of the enzyme are maintained in this model structure: adenine N1 with Thr57 and N6 with Glu59, and ribose O2′ with Glu156. Other contacts are different due to the changed positions of several side chains. In particular, adenine contacts with His353 and ribose contacts with Lys186 and Asp190 are not found in the open form of the enzyme.

For AdoHcy, the 100 lowest-energy structures exhibited rms deviations of 0.7−3.0 Å for the adenine ring, compared to the adenine position of 3′-keto-DHCeA in the overlaid catalytic domain of the closed form. In the Ado moiety of AdoHcy of the lowest-energy structure, a hydrogen bond network similar to that for Ado itself was observed. The Hcy tail makes contacts with His55, Cys79, Asn80, and Asp131. Met358 is found in contact with the adenine moiety in our model. This residue was not involved in contacts with ligands in any of our other simulations presented in this paper.

Docking of Ado and AdoHcy to the Closed Form. The AutoDock program was able to locate the Ado binding site in the closed form of human AdoHcy hydrolase (Table 2). The docking produced a small number of clusters, compared to the docking of Ado to the open form of AdoHcy hydrolase (Table 2). One hundred twenty-eight runs yielded 22 clusters, with a docking energy of −62.0 kcal/mol for the lowest-

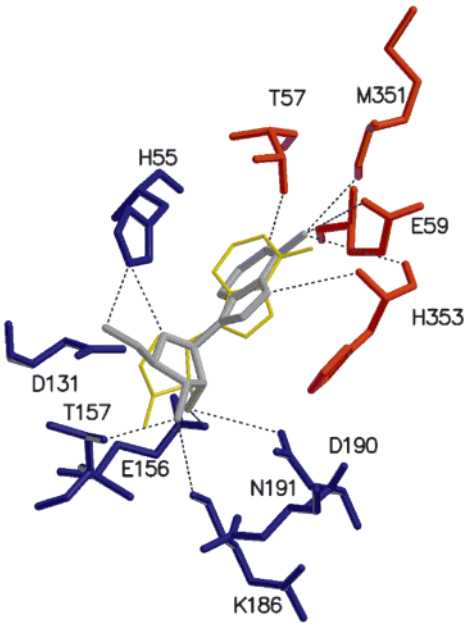

FIGURE 3: Docked structure of Ado (gray), obtained by AutoDock, in the binding site of the closed form of AdoHcy hydrolase. The location of 3′-keto-DHCeA (yellow) in the crystal structure is shown for reference. The residues involved in the binding of the adenine and ribose moieties of the docked inhibitor are indicated in red and blue, respectively. Dotted lines denote possible interactions across distances of <4.0 Å.

energy cluster. In this docked model, residues Leu54, Thr57, Glu59, Met351, His353, and Phe362 are involved in binding the adenine ring (Figure 3), and 2′- and 3′-hydroxyl groups are making H-bonds to Glu156, Lys186, and Asp190 of the enzyme. These results are consistent with previous studies (*7*). However, the ribose ring is tilted about 30° in the Ado-docked model, compared with the cyclopentene ring of 3′-keto-DHCeA in the 1A7A structure. In this model, the 3′-hydroxyl group of Ado forms a good hydrogen bond with Oγ of Thr157 and O4′ interacts with His55 and Asp131, while His55 participates in the binding of the 5′-hydroxyl group of the ribose moiety in Ado (Figure 3). The distance between H4′ of the ribose ring and Oδ of Asp131 is 2.7 Å.

The specific binding site for Ado was also explored using CHARMM. The CHARMM simulation produced a result very similar to that with AutoDock. The lowest-energy structure was repeated 437 times among the 1000 minima produced by simulated annealing. In this structure, the adenine ring was within 1.6 Å (rms deviation) of the 1A7A crystal coordinates. The adenine ring occupies essentially the same location as it does in the adenine moiety of 3′-keto-DHCeA of the crystal structure. The relatively large rms deviation is due to a tilt of the ring, like that seen in the AutoDock model (see Figure 3). The CHARMM model presented the same hydrogen bond pattern as observed in the AutoDock model. Hydrogen bonds to the adenine ring were close to optimal, while most hydrogen bonds to the ribose were too long.

In the simulation of docking of AdoHcy to the enzyme, the energy-minimized structure of computer-built AdoHcy was used as the starting point for the docking searches. The initial searches were carried out with AutoDock, producing 86 clusters of 128 runs. The best docked structure placed AdoHcy in the general active site of the enzyme (Figure 4A). In this model, Asn80, Asp131, and Asp134, which are located in the middle of the entry tunnel described by Turner et al. (*7*), were identified as the most important residues involved in binding of the Hcy moiety. It should be noted that the Ado moiety is shifted ~1 Å in the direction of the Hcy tail, compared to the crystal structure with 3′-keto-DHCeA as the ligand.

The CHARMM program, which allows full ligand flexibility, was used to perform further docking simulations, using the best AutoDock structure as the starting model. The best binding mode of the flexible substrate AdoHcy is illustrated in Figure 4B. In this model, the Hcy tail is hydrogen bonded to residues Asn80 and Asp131. Residues His55, Cys79, and Leu344 are also identified as interaction partners in the Hcy tail binding, forming nonspecific contacts. The adenine moiety is located in a position more similar to that of 3′-keto-DHCeA in the crystal structure than is the case for the AutoDock structure, while the Hcy tail moves away from Asp134. With respect to the conformation of

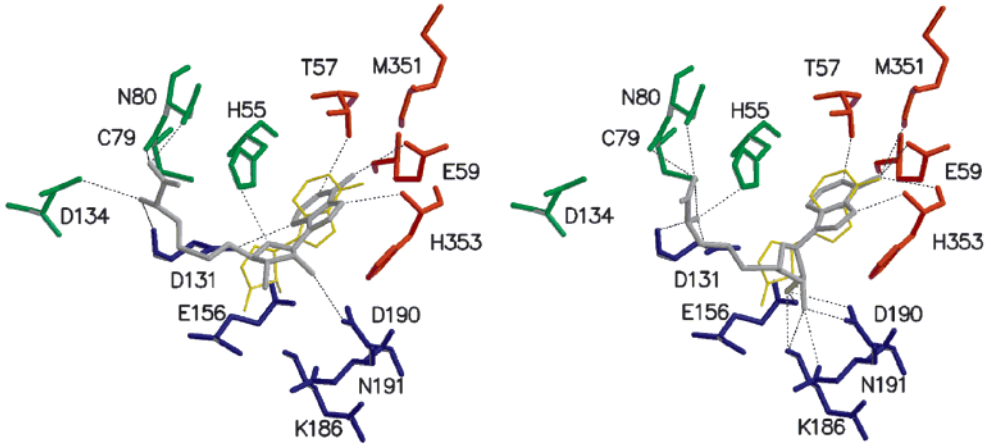

FIGURE 4: AdoHcy binding models in the closed form. (A) The lowest-energy structure produced by AutoDock and (B) the strained conformation predicted by CHARMM simulation. The crystal structure location of 3′-keto-DHCeA (yellow) is shown for reference. The residues involved in the binding of the adenine, ribose, and Hcy moieties of the docked inhibitor are depicted in red, blue, and green, respectively. Dotted lines denote possible interactions across distances of <4.0 Å.

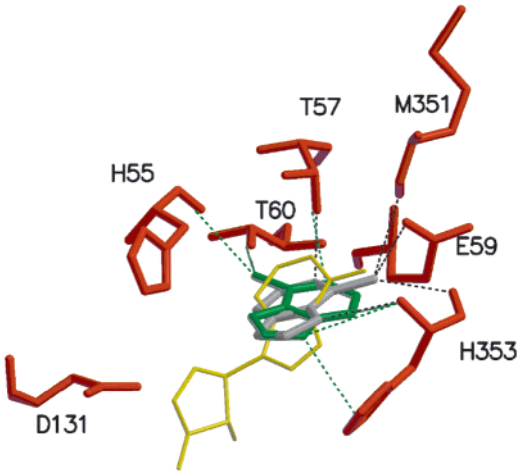

FIGURE 5: Adenine docking solutions in the low-energy group. The first-ranked (lowest-energy) and second-ranked binding modes are shown as green and gray sticks, respectively. The location of 3′-keto-DHCeA (yellow) in the crystal structure is shown for reference.

AdoHcy, CHARMM calculations indicate that favorable interactions with the protein induce ~10 kcal/mol of internal strain in AdoHcy molecule, mostly due to angle deformation. This internal energy increase is compensated by favorable nonbonded interactions with the protein. Thus, thanks to the ligand flexibility in the CHARMM simulation, the docked structure of the adenine ring of AdoHcy is closer than the AutoDock result to the crystal coordinates of this moiety in the 3′-keto-DHCeA crystal structure, probably because AutoDock allows for only dihedral deformation. The internal strain induced in the substrate by binding may reduce the reaction barrier and enhance the catalytic rate. The rms deviation of the adenine ring between the CHARMM complexes and the crystal structure was ~1.6 Å.

Docking of Adenine and 3′-Keto-DHCe to the Closed Form. The AutoDock simulation of adenine docking to the closed form of human AdoHcy hydrolase produced 10 solution clusters (Table 2). The lowest-energy structures within each of the first two low-energy clusters exhibit low docking energy, with adenine in the adenine ring binding site of the crystal structure (*7*). However, the docked adenine rings in the two clusters exhibit markedly different orientations. In the first (lowest-energy) docked structure, the ring is rotated by ~180° compared with the adenine ring of 3′-keto-DHCeA in the crystal structure, while the second docked structure has the same orientation as shown by the 1A7A crystal structure (rms deviation of 1.27 Å from the position of the adenine fragment; Figure 5). In these two docked models, the protein residues involved in the interactions are identical and the same number of hydrogen bonds was observed. These two solutions had similar docking energies (−37.1 and −36.7 kcal/mol, respectively), and both were considered as possible binding models. In contrast to adenine, the docking of 3′-keto-DHCe, the complementary fragment of 3′-keto-DHCeA, produced 33 clusters, remarkably more than that produced in the adenine docking (Table 2). The rms deviation of the low-energy docked structures from the position of the 3′-keto-DHCe fragment of 3′-keto-DHCeA in the crystal structure is in the range of 3−5 Å.

DISCUSSION

Validation of the Methods. The crystal structure of 3′-keto-DHCeA bound to the closed form of human AdoHcy hydrolase was used to test our docking protocols (*7*). In the crystal structure, 3′-keto-DHCeA is deeply engulfed in a closed active site as a result of the closure of the mobile substrate-binding domain against the cofactor-binding domain. Only residues from the catalytic domain and the hinge, and a water molecule, are involved in 3′-keto-DHCeA binding. To allow 3′-keto-DHCeA to move into the active site during the docking processes, the NAD^+-binding domain, which is not directly involved in the interaction with the substrate, was removed.

Both the AutoDock and CHARMM docking simulations of 3′-keto-DHCeA were successful with the docking methods described in the method section. The AutoDock simulation produced a small number of low-energy clusters, indicating a high specificity of 3′-keto-DHCeA binding in the closed form of AdoHcy hydrolase. In addition, the rms deviation between the first ranked solution and the crystal structure was only 0.8 Å. In the CHARMM simulations of 3′-keto-DHCeA, the optimal structures were repeated 565 times and the rms deviation is 1.5 Å from the crystal structure. These results demonstrated that both AutoDock and CHARMM programs, using very different approaches, are able to functionally reproduce the situation in the crystal structure.

Since Thr57, Glu59, Glu156, Gln181, Lys186, and Asp190 of AdoHcy hydrolase are the key residues with side chains involved in 3′-keto-DHCeA binding, mutations of these residues should affect the binding specificity of the inhibitor. To validate the ability of the docking methods to detect these specific interactions, 3′-keto-DHCeA was docked into the active site of the mutant proteins T57A, E59A, E156A, N181A, K186A, and D190A, generated by computational mutagenesis. An experimental mutagenesis study of these protein residues has also been carried out. In the computational study, the number of clusters produced in the docking experiments with the mutants was always greater (18−51; Table 1) than 16, the number of clusters produced by the wild-type docking simulation, indicating a decreased binding specificity induced by mutations of the amino acids in the substrate-binding motif. This result is consistent with our experimental data, which will be published separately.

The results indicated that our procedure provides a functional approach to the binding mode of various ligands and some information about residues involved in catalysis and inhibition.

Substrate Binding in the Open Form of AdoHcy Hydrolase. As mentioned earlier, in the crystal structure determined for rat liver AdoHcy hydrolase, the enzyme is in the open form and has neither substrate nor inhibitor in the catalytic site. To address the modes of binding of Ado and AdoHcy to the open form of the enzyme, a docking simulation of each substrate was performed with the rat enzyme as the target protein (Table 2). The AutoDock docking runs for each ligand produced a large number of clusters; 128 runs yielded 106 clusters for Ado and 125 for AdoHcy out of a maximum of 128. The docked ligands exhibited a wide range of rms deviations (5−33 Å).

The large number of different docking structures obtained in the AutoDock simulations appears to indicate an inability of the catalytic site in the open form of the enzyme to recognize and specifically bind the substrates Ado and AdoHcy. To examine possible reasons for this deficiency, we constructed a rough superimposition of the substrate-binding domains in the open and closed forms. The interact-

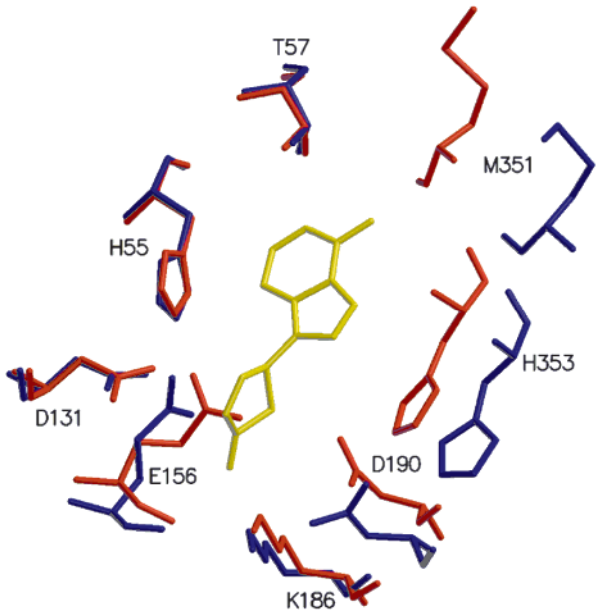

FIGURE 6: Superimposed substrate binding sites in two forms (open, blue; closed, red). The 1A7A crystal structure of 3′-keto-DHCeA (yellow) is from the closed form and is shown for reference.

ing residues in the substrate-binding site of the closed form are from the catalytic domain and the hinge part. Therefore, protein segments form residue 2 through 193 and 343 through 404, which contain all of the interacting residues in the substrate binding site of the closed form, were selected and subjected to a least-squares superimposition. The rms deviation between the superimposed structures is 0.6 Å, and the result is shown in Figure 6. The open form (blue color) of the enzyme has an "exploded" structure of the binding site such that the interacting residues are moved to points so distant (in some cases, as much as 5 Å) from the their positions in the closed form that simultaneous satisfaction of more than one or two of the stabilizing interactions present in the closed form of the enzyme is impossible. This situation suggests that substrate binding and conversion of the enzyme from the open to closed form must be coupled processes, as suggested by earlier studies of fluorescence anisotropy relaxation (*9*).

To test whether the lack of specificity found in the AutoDock simulations could be an artifact of the small number of adjustable degrees of freedom in the ligand and enzyme in this procedure, CHARMM simulations were performed with a fully flexible ligand and a partially flexible protein. In these CHARMM simulations, the protein side chains in the active site were allowed to reorient and a series of atomic constrains on the adenine skeleton ($f = 0.01$, 0.05, 0.1, and 0.5 kcal mol^{-1} Å^{-2}) were tested. A wide range of possible docked structures of Ado and AdoHcy was found in the general area of the active site. This is in general agreement with AutoDock docking results and indicates a low specificity for substrate binding in the open form. In the case of Ado, some of the lowest-energy structures are within 1 Å (rms deviation) of the position of 3′-keto-DHCeA in the crystal structure, while others have alternative orientations of the adenine ring. The minimum energy structures of Ado and AdoHcy from CHARMM simulations have binding orientations similar to that of the crystal structure of 3′-keto-DHCeA in the closed form of human AdoHcy hydrolase (*7*), although fewer interactions between the ligand and the protein were observed in the open form. Thus, the structures of Ado and AdoHcy bound to the open form are characterized by partial satisfaction of the contacts of the adenine and ribose parts of the system. However, the contacts of the Hcy tail of AdoHcy are essentially identical in the closed and open form models. In addition, it appears that the adenine moiety can form more optimal hydrogen bonds than the ribose. This result is in agreement with the finding first suggested by Porter et al. that the adenine is the recognition element for substrate binding (*24*).

Modes of Binding of Ado and AdoHcy to the Closed Form of Wild-Type Human AdoHcy Hydrolase. Since the modes of binding of the natural substrates Ado and AdoHcy to the closed form of wild-type AdoHcy hydrolase have not been directly observed in crystal structures, we simulated the binding of Ado and AdoHcy to the closed form (Table 2). The only available crystal structure that contains the native substrate is the rat AdoHcy hydrolase mutant D244A, which contains 1.0 mol of Ado and 0.5 mol of NADH cofactor per mole of subunit, with the protein in a closed conformation [PDB entry 1D4F (*21*)]. As in the case of human AdoHcy hydrolase, the AutoDock and CHARMM programs produced consistent results in locating the Ado binding site. Figure 3 shows the docked structure of Ado in the closed form of human AdoHcy hydrolase. In this model, the residues involved in interaction with the adenine ring are Thr57, Glu59, Met351, His353, and Phe362, which is consistent with both the crystal structures of human AdoHcy hydrolase and rat AdoHcy hydrolase mutant D244A (*7*, *21*). The ribose 2′- and 3′-hydroxyl groups are making H-bonds to the enzyme through the same residues (Glu156, Lys186, and Asp190) as observed in the crystal structure of the 3′-keto-DHCeA complex. However, the ribose ring is tilted about 30° in the Ado-docked model, compared with the cyclopentene ring of 3′-keto-DHCeA in the crystal. This difference was not inconsistent with structural differences between 3′-keto-DHCeA and Ado. The ring orientation observed here allows the 3′-hydroxyl group (not present in 3′-keto-DHCeA) to form a good hydrogen bond with Oγ of Thr157. Also, in this orientation, O4′ may interact with His55 and Asp131. His55 also participates in the binding of the 5′-hydroxyl group (not present in 3′-keto-DHCeA) of the ribose moiety in Ado**,** indicating a key role in the elimination and addition of water for the oxidized intermediate 3′-keto-Ado during the catalysis. The calculated distance between H4′ of the ribose ring and Oδ of Asp131 is 2.7 Å. With the consideration of the side chain orientations, Asp131 becomes the best candidate as the 4′-hydrogen receptor in the elimination reaction. In the model complexes, the hydrogen bonds to the adenine ring were close to optimal, while most hydrogen bonds to the ribose were too long. Like the docking results of Ado and AdoHcy in the open form, this indicates that adenine is the main recognition element in substrate binding.

The docking of AdoHcy to the closed form of the enzyme was not as straightforward as that of Ado. The larger AdoHcy molecule is more flexible than Ado, and this feature makes the docking of AdoHcy more challenging than that of Ado. It was impossible to predict a probable conformation for AdoHcy before the docking runs, so we used the energy-minimized structure of AdoHcy as the starting point for the docking searches. The best-docked structure from the AutoDock runs is in the general active site of the enzyme (Figure 4A). In this model, Asn80, Asp131, and Asp134,

which are located in the middle of the substrate entry tunnel (*7*), were identified as the most important residues involved in Hcy tail binding. However, the Ado moiety is shifted ~1 Å in the direction of the Hcy tail, compared to the crystal structure of 3′-keto-DHCeA (*7*). Because of this apparent disagreement with the crystal structure, we extensively searched nearby regions of the catalytic and cofactor-binding domains visually for possible candidate structures that might accommodate the Hcy moiety. No such area was found in the general active site region, other than the Hcy binding site identified by AutoDock. Assuming that Asn80, Asp131, and Asp134 should be the correct binding partners, we concluded that AdoHcy must bind in a strained conformation, allowing the adenine moiety to stay in the most favorable binding site, which has been identified in the 3′-keto-DHCeA crystal structure. This could be accomplished by straining the bond angles and/or bond lengths of the energy-minimized AdoHcy structure, which had been optimized for an isolated molecule. To test the molecular distortion, the CHARMM program, which allows full ligand flexibility, was used to perform further docking simulations, using the best AutoDock structure as the starting model.

The CHARMM results were in excellent agreement with a strained ligand structure. The best binding mode of the flexible substrate AdoHcy is found when weak constraints were applied to restrain the adenine ring to the general area of the binding site (Figure 4B). In this model, Ado interacts with the same residues that are observed in the 1A7A crystal structure. The Hcy tail is hydrogen bonded to residues Asn80 and Asp131. Residues His55, Cys79, and Leu344 were also identified as interaction partners in Hcy tail binding, forming nonspecific contacts. With respect to Hcy tail binding, CHARMM and AutoDock results are similar, although they differ in the details. In the CHARMM calculations, residue Asp134 (suggested by AutoDock) does not interact directly with the Hcy tail when only weak constraints are applied to keep the adenine ring close to its position in the complex derived with AutoDock. In this case, the adenine moiety is located in a position more similar to that in the 3′-keto-DHCeA crystal structure, while the Hcy tail moves away from Asp134. On the basis of CHARMM calculations, ~10 kcal/mol of internal strain in AdoHcy was induced by the favorable interaction between the ligand and the protein, mostly due to angle deformation. This is compensated by favorable nonbonded interactions between the adenine moiety of AdoHcy and the protein (see below for details). We believe this straining process may be important for the catalytic function of AdoHcy hydrolase, as destabilizing the substrate leads to a lowering of the energy barrier for the elimination reaction.

Identification of the Recognition Elements in the Substrate. Porter and Boyd suggested that the interactions of the adenine moiety of the substrate with AdoHcy hydrolase are the major contribution to the stability of the initial complex between Ado or AdoHcy and this enzyme (*24*). As mentioned above, our docking results for the substrates in the close from confirmed that adenine might be the main recognition element in substrate binding.

Evaluating the binding specificity of substructures of a substrate is a useful strategy for evaluating the contributions of the substructures to enzyme−substrate recognition (*20*). In our computational study of AdoHcy hydrolase presented here, this strategy was employed to address the identity of the recognition element of the substrate by docking the substructures adenine and 3′-keto-DHCe separately into the closed form of human AdoHcy hydrolase (Table 2). The 128 AutoDock docking runs of adenine produced 10 clusters, while the same number of runs of 3′-keto-DHCe produced 33 clusters, indicating a significant difference between the binding specificities of these two molecules. Because a smaller number of clusters reflects a higher binding specificity, we conclude that AdoHcy hydrolase has a higher specificity for adenine than it does for 3′-keto-DHCe. In addition, the rms deviations of the low-energy solutions of the adenine docking are <1.3 Å, while those of 3′-keto-DHCe docking are >3.0 Å. Therefore, our docking studies suggest that the adenine moiety of the substrate may be the main recognition element for substrate binding to AdoHcy hydrolase, while the major role of the ribose moiety may be in the oxidation−reduction reaction, rather than in substrate recognition.

The computational and experimental mutagenesis studies described in Validation of the Methods also confirmed this conclusion (Table 1). On the basis of our previous crystallographic studies, we have suggested that the side chains of Thr57 and Glu59 directly interact with the adenine ring of the substrate, while Glu156, Gln181, Lys186, and Asp190 are the important residues involved in interaction with the ribose moiety (*7*). In the current computational study, all the residues interacting with the substrate were mutated to alanine and 3′-keto-DHCeA was docked into the active sites of these mutants.

When the mutant enzymes T57A and E59A were used as the docking targets, the numbers of clusters that were produced were significantly larger than the number produced using wild-type AdoHcy hydrolase as the target (Table 1). This result suggests the important role of Thr57 and Glu59, residues that bind the adenine, in defining the substrate binding specificity. In contrast, the simulations of docking of 3′-keto-DHCeA to the mutants involving substitutions of the residues interacting with the ribose moiety produced results similar to those for wild-type AdoHcy hydrolase, although they generated slightly more than 16 clusters. There was no significant difference between the number of the clusters of the wild type and the mutants, suggesting that they all are very similar with the wild-type enzyme in terms of substrate binding specificities. This result indicates that the binding of the ribose moiety of a substrate is not critical for high-specificity binding of the substrate as a whole. An experimental mutagenesis study of these protein residues has also been carried out. The substrate affinities detected for the mutant proteins E156A, E181A, K186A, and D190A were similar with those for the wild-type enzyme, although some of the mutants exhibit a loss of activity (a finding that will be published in a separate paper). All these results suggest that the adenine ring plays the major role in substrate binding to AdoHcy hydrolase.

Modes of Binding of Adenine to the Closed Form of AdoHcy Hydrolase. It is thus of interest to look at the hitherto unknown modes of binding of adenine itself to the closed form of AdoHcy hydrolase. The AutoDock docking runs for adenine produced 10 solution clusters. The clusters fall into two groups. The first- and second-ranked clusters form a low-energy group, and the remaining clusters are at higher (>5 kcal/mol) energy. Because the difference in energy between the two groups was significant, only the low-energy

group members were considered as possible binding structures. In the low-energy group, each of the two clusters contained a number of solutions: 38 in the first and 62 in the second cluster. An inspection of the representative solutions of the two clusters shows them located in the adenine ring binding site of crystal structure 1A7A. However, the docked adenine rings in the two clusters exhibit markedly different orientations. In the first cluster, the ring is flipped by ~180° (Figure 5), compared with the adenine ring of 3′-keto-DHCeA in the crystal structure, while the second cluster contains solutions having the same orientation as the crystal structure. In these two docked models, the protein residues involved in the interactions are identical, although distinct hydrogen bond networks were observed. Since these two solutions had similar docking energies (−37.1 and −36.7 kcal/mol, respectively), it was difficult to distinguish from the energy values which solution is the preferable one. On the basis of the solution numbers in each cluster, the second one may have a higher probability of occupancy than the first.

Summary. In this work, we have simulated the mode of binding of Ado and AdoHcy to the open form of AdoHcy hydrolase, and adenine, Ado, and AdoHcy binding to the closed form of the enzyme. In the open form, the substrate binds to the enzyme nonspecifically, consistent with an exploded structure for the binding site. In the closed form, Ado binds to the enzyme by interacting with the residues identified in the crystal structures. His55 in the docked model appears to participate in the elimination of water from Ado. In the same reaction, Asp131 removes a proton from the 4′ position of the substrate after the oxidation−reduction reaction in the enzyme. The results of our simulations of AdoHcy binding indicate that the Hcy tail of AdoHcy binds to the closed form of AdoHcy hydrolase in a strained conformation, which is important to catalysis because it lowers the transition state energy. His55, Cys79, Asn80, Asp131, Asp134, and Leu344, which are at the middle region of the substrate entry tunnel, were identified as possible interaction partners for Hcy tail binding. The adenine part was identified as the major recognition element for the substrate binding to AdoHcy hydrolase, while the ribose moiety is important for oxidation and reduction ability rather than binding recognition. Two possible orientations were observed for an adenine molecule docked to the closed form of AdoHcy hydrolase.

The results from the current computational study complement the existing experimental data. This study uncovered some new and important information for AdoHcy hydrolase, which provides a better understanding of the catalytic mechanism of this biologically and pathologically important enzyme. The combination of AutoDock and CHARMM appears to be an excellent docking strategy for the study of AdoHcy hydrolase. It may be used for the future studies of this enzyme. It may also be applied to other enzymes of interest.

ACKNOWLEDGMENT

We thank Dr. P. Lynne Howell for insightful discussions. Y.H. thanks Dr. Teruna J. Siahaan for full support during the course of these studies.

REFERENCES

1. Turner, M. A., Yang, X., Yin, D., Kuczera, K., Borchardt, R. T., and Howell, P. L. (2000) *Cell Biochem. Biophys. 33*, 101−125.
2. De Clercq, E. (1987) *Biochem. Pharmacol. 36*, 2567−2575.
3. Yin, D., Yang, X., Borchardt, R. T., and Yuan, C.-S. (2000) in *Biomedical Chemistry: Applying Chemical Principles to the Understanding and Treatment of Disease* (Torrence, P. F., Ed.) pp 41−71, John Wiley & Sons, New York.
4. Henderson, D. M., Hanson, S., Allen, T., Wilson, K., Coulter-Karis, D. E., Greenberg, M. L., Hershfield, M. S., and Ullman, B. (1992) *Mol. Biochem. Parasitol. 53*, 169−183.
5. Bitonti, A. J., Baumann, R. J., Jarvi, E. T., McCarthy, J. R., and McCann, P. P. (1990) *Biochem. Pharmacol. 40*, 601−606.
6. Chambers, J. C., Seddon, M. D., Shah, S., and Kooner, J. S. (2001) *J. R. Soc. Med. 94*, 10−13.
7. Turner, M. A., Yuan, C. S., Borchardt, R. T., Hershfield, M. S., Smith, G. D., and Howell, P. L. (1998) *Nat. Struct. Biol. 5*, 369−376.
8. Hu, Y., Komoto, J., Huang, Y., Gomi, T., Ogawa, H., Takata, Y., Fujioka, M., and Takusagawa, F. (1999) *Biochemistry 38*, 8323−8333.
9. Yin, D., Yang, X., Hu, Y., Kuczera, K., Schowen, R. L., Borchardt, R. T., and Squier, T. C. (2000) *Biochemistry 39*, 9811−9818.
10. Morris, G. M., Goodsell, D. S., Huey, R., and Olson, A. J. (1996) *J Comput.-Aided Mol. Des. 10*, 293−304.
11. Brooks, B. R., Bruccoleri, R. E., Olafson, B. D., States, D. J., Swaminathan, S., and Karplus, M. (1983) *J. Comput. Chem. 4*, 187−217.
12. Heine, A., Stura, E. A., Yli-Kauhaluoma, J. T., Gao, C., Deng, Q., Beno, B. R., Houk, K. N., Janda, K. D., and Wilson, I. A. (1998) *Science 279*, 1934−1940.
13. Stoddard, B. L., and Koshland, D. E., Jr. (1992) *Nature 358*, 774−776.
14. Walters, W. P., Stahl, M. T., and Murcko, M. A. (1998) *Drug Discovery Today 3*, 160−178.
15. MacKerell, A. D., Jr., Wiórkiewicz-Kuczera, J., and Karplus, M. (1995) *J. Am. Chem. Soc. 117*, 11946−11975.
16. MacKerell, A. D., Jr., Bashford, D., Bellott, M., Dunbrack, R. L., Jr., Evanseck, J. D., Field, M. J., Fischer, S., Gao, J., Guo, H., Ha, S., Joseph-McCarthy, D., Kuchnir, L., Kuczera, K., Lau, F. T. K., Mattos, C., Michnick, S., Ngo, T., Nguyen, D. T., Prodhom, B., Reiher, W. E., Jr., Roux, B., Schlenkrich, M., Smith, J. C., Stote, R., Straub, J., Watanabe, M., Wiórkiewicz-Kuczera, J., Yin, D., and Karplus, M. (1998) *J. Phys. Chem. B 102*, 3586−3616.
17. Kraulis, P. J. (1991) *J. Appl. Crystallogr. 24*, 946−950.
18. Bacon, D. J., and Anderson, W. F. (1988) *J. Mol. Graphics 6*, 219−220.
19. Merritt, E. A., and Murphy, M. E. P. (1994) *Acta Crystallogr. D50*, 860−873.
20. Miller, B. G., Snider, M. J., Wolfenden, R., and Short, S. A. (2001) *J. Biol. Chem. 276*, 15174−15176.
21. Komoto, J., Huang, Y., Gomi, T., Ogawa, H., Takata, Y., Fujioka, M., and Takusagawa, F. (2000) *J. Biol. Chem. 275*, 32147−32156.
22. Minke, W. E., Diller, D. J., Hol, W. G., and Verlinde, C. L. (1999) *J. Med. Chem. 42*, 1778−1788.
23. Frisch, M. J., Trucks, J. W., Head-Gordon, M., Gill, P. M. W., Wong, M. W., Foresman, J. B., Johnson, B. J., Schlegel, H. B., Robb, M. A., Replogle, E. S., Gomperts, R., Andres, J. L., Raghavachari, K., Binkley, J. S., Gonzalez, C., Martin, R. L., Fox, D. J., Defrees, D. J., Baker, J., Stewart, J. J. P., and Pople, J. A. (1992) *Gaussian 92*, revision C, Gaussian, Inc., Pittsburgh, PA.
24. Porter, D. J. T., and Boyd, F. L. (1991) *J. Biol. Chem. 266*, 21616−21625.

BI015690D